International Journal of Scientific Research and Engineering Development-– Volume 5 Issue 5, Sep- Oct 2022

Available at www.ijsred.com

RESEARCH ARTICLE OPEN ACCESS

# Nanostructured CuO and G-CuO : Combined Experimental and Theoretical Studies

Dr.E.Bharathi[*1], S.Ravikumar[*2], Dr.S.Senthilvelan[*3]

([*1]Assistant professor, Chemistry, Joseph Arts and Science College, Thirunavallur, cuddalore, Tamilnadu, India )

([*2] Research Scholar, Physics, Anna University, Chennai, India)

([*3] Associate Professor, Chemistry, Annamalai University, Annamalai nagar, Chidambaram, India)

## I. ABSTRACT

The G -CuO composite is synthesized by simple sol-gel process. Guanine interactions with CuO nanocluster of various sizes have been investigated. The geometric and electronic structures of CuO and G-CuO have been evaluated by using DFT, B3LYP/ LANL2DZ method. The different clusters were optimized to study the HOMO-LUMO energy gap and binding energy of CuO and G-CuO. The electronic structures of clusters were discussed in terms of HOMO-LUMO energy gap and DOS states. Mulliken charges are computed. The prepared G-CuO and CuO nano composites have been characterized by FT-IR, HR-SEM, EDAX and FT-RAMAN analytical techniques. Their nanostructure and morphologies were characterized by High resolution scanning electron microcopy. This shows that exist of nanostructures of CuO and G-CuO. The optical properties of nanostructures were evaluated by Uv-Vis Spectroscopy. The observational data of microscopic and spectroscopic is also discussed for realizing the G-CuO interactions. In all the case the observational results are equated with the DFT computation.

Keywords: **Spectroscopic studies; Nano cluster; DFT; HOMO-LUMO; binding energy;**

## I. INTRODUCTION

Among several metal nanoparticles, copper (Cu) and copper oxide ($Cu_2O$) nanoparticles have appealed since copper is one of the significant metal in easier obtainable [1.] Its significant involvement has been paid attention along with copper nanoparticles due to their remarkable catalytic, mechanical, optical, and electronic properties [2, 3]. The transition metal oxides are belongs to important family of semiconductor device. Copper oxide (CuO) is one of the significant p-type semi- conductor (narrow band gap of 1.4 eV) among the transition metal oxides[4] with individual properties, which makes it suitable for the applications in gas sensors,[5] photo catalysts,[6]and lithium ion batteries.[7] Electrochemical sensors,[8] size and shape controlled [9–10] Nucleic acids recommend the Analytical chemist an effective device because of the detection of important compounds [11]. purines

  

and pyrimidine bases in DNA form hydrogen bonds among them with their relevant complementary base are plays a essential function in biologic systems and prove to oxidative stress.[12.]

Copper oxide nanoparticles are involved generally in bio medical applications such as biocide and antimicrobial activities.[13,14] Therefore, the production method engaged a well-designed genetic characteristics. The metal oxide nano particles like CuO, $Fe_3O_4$, $TiO_2$, and ZnO are used as latest new antibacterial agents. Because of low toxicity to the human cells [15], Its dimension suitable for inhibition for an extensive series of bacteria's, and capability towards prevent construction of bio film [16] smooth eradicate spores [17] products of skincare [18] biomedical [19] and food additive industries [20].

In this work, we prepared CuO nano particles (nps) and guanine doped CuO (nps). Bio physical interaction has been studied by theoretical and Experimental analysis viz IR and Raman spectroscopy. DFT results have done to study properties of geometry, structure with electronic and vibrational details. The guanine interaction on the Clusters of CuO (G-CuO) were analyzed in detail by B3LYP/Lanl2dz method.The present work has also on expressed, how CuO nps interacting with active site viz N, O and $NH_2$ in the guanine molecule. From the optimized geometry, the DOS spectrum was simulated. The high value of Mulliken energy indicates that weak force between Cu-N atoms of the guanine adsorbed CuO nps. According to the above discussion, it is found as bio-nano interactions. The observed results are also incorporated the above adsorption phenomenon. Finally, we report that physisorption force can claim in the biomedical applications.

## II. EXPERIMENTAL

### 1) Materials and Methods

Copper chloride ($CuCl_2.2H_2O$), Sodium hydroxide (NaOH), glacial acetic acid ($CH_3COOH$) and guanine ($C_5H_5N_5O$) were the assured AR grade used from Sigma Aldrich. All the apparatus were washed through chromic acid and followed with acetone and lastly dried at 100°C an oven.

### 2) Preparation of CuO

The aqueous solution of $CuCl_2.2H_2O$ (0.1 M) was transferred to cleaned 250 ml beaker. 2 ml of glacial acetic acid was added together to an over aqueous solution and heated near 100 °C with constant stirring. 4M sodium hydroxide (NaOH) was added to above heated solution until the pH reaches to 7. Green colour of the solution was turned to black and the huge amount of black precipitate is obtained. The above precipitate is centrifuged and washed 2-3 times with a deionised water. The obtained precipitate was dehydrated in air for a day. The obtained material was calcined at $420^0$C for 1 h, to get CuO nanoparticles. This powder was further used for guanine adsorption and characterizations of CuO

  

nanoparticles. Preparations of Nano crystalline (NC) CuO reactions are implicated in the preparation are shown below.

### 3) Procedure of guanine adsorption over the CuO and(G–CuO ) nanoparticles

The CuO nanoparticles and guaranteed guanine molecule were isolated by using 50 ml conductivity water. The above mixture was sonicated for 30 min and separated. The above precipitate was dehydrated at 100 $^{o}$C for 6h. After ground well the final product of G-CuO nano materials to get a G–CuO composite. This G–CuO composite was characterized by using techniques of SEM with EDX, FT-IR and FT-RAMAN analysis.

### 4) Computational contingent

By using the method of Becke, three-parameter, Lee–Yang–Parr (B3LYP), Gaussian 03Wsoftware was used to study the simulate optimization of the ground state geometry of CuO and G-CuO cluster.[21]HOMO-LUMO calculations for different geometrically optimized CuO and G-CuO clusters are carried out using Gauss sum 2.2 packages [22]Chemcraft 1.6 software was used to visualizing the structure of molecule.[23]

### 5) Characterization Techniques

The synthesized compounds were analyzed by SHIMADZU FT-IR spectrometer with in KBr pellet. FT-Raman spectra was recorded with an intact microscope of RFs27 fitted out of Raman system along 1024 256 pixels have a liquefied Nitrogen cooled germanium detector.15 MW preserved to defect that the sample heating as intense. An achievement time of 185 recover were establishing to take each spectrum. Scanning electron microscopy and elementary dispersive X-ray analysis were recorded at 25 1C on FEI quanta FEG 200 instrumentation, accompanying EDAX analyzer. The little amount of prepared sample was placed on carbon coated. For Ultraviolet and visible light absorption spectroscopy range of 600-200 nm with SHIMADZU UV-1650PC was used with the help of the 10mm optical path length of quartz cell.

## III. RESULTS AND DISCUSSION SECTION

### 1) Optimized cuo clusters and its electronic properties

The optimized structures of CuO clusters are shown in **Fig. 1.** (a)$Cu_2O_2$, (b)$Cu_3O_3$ (c) $Cu_4O_4$ (R) and (d)$Cu_4O_4$ (w). In CuO clusters of HOMO–LUMO energy gap value, scaled energy and binding energy are calculated and shown in **Table.1**. The energy gap (Eg = $E_{LUMO}$ - $E_{HOMO}$) of the CuO clusters were shown in **Fig. 2.** It represents the total density of states (DOS). The Eg values of $Cu_2O_2$, $Cu_3O_3$, $Cu_4O_4$ (R) and $Cu_4O_4$ (w) are **2.45**, **0.03**, **1.36**, and **1.63**eV. Binding energy (BE) is one of the parameters to analyze the stability of the cluster. The binding enegy value of CuO cluster was calculated by the equation EB = $[(n*E_{Cu}+ n*E_O- E*_{(CuO)})/n]$ [24], n

  

represents number of CuO atoms in the cluster. E (Cu) is the energy of Copper; E (O) is the energy of oxygen. The binding energy values of $Cu_2O_2$, $Cu_3O_3$, $Cu_4O_4$ (R) and $Cu_4O_4$ (w) are 6.12, 7.34, 7.75 and 7.21 eV as given **Table; 1.** The $Cu_2O_2$ cluster energy gap value is higher when compared to $Cu_4O_4$ (R), $Cu_3O_3$ and $Cu_4O_4$ (W) clusters. According to the value of HOMO-LUMO energy gap value the $Cu_2O_2$ structure is most favored electronic structure. But the most stable cluster as $Cu_4O_4$(R).This is clearly identified from **Fig; 6.** The scaled energy, calculated by $E_S$=E/N, Where the total energy is represented as E and N is denoted for number of atoms present in the cluster. The CuO cluster bond length series are $R_{(CuO)}$ from 1.77-1.99 Å. CuO bond shows ionic character because of charge transfer between the bond Cu and O atom.

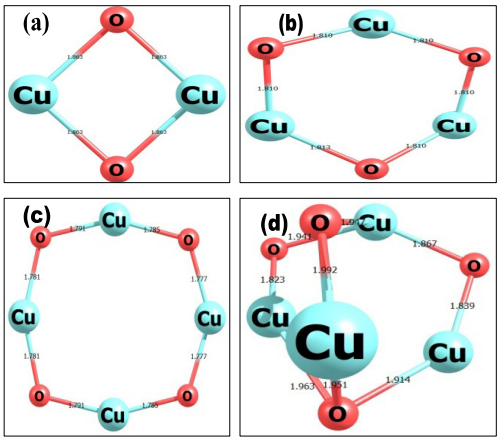


**Fig:1 Optimized structure of CuO Clusters (a) $Cu_2O_2$ (b) $Cu_3O_3$ (c) $Cu_4O_4$ (R) (d) $Cu_4O_4$ (w)**

**2) Models of guanine adsorption on CuO clusters (G-CuO), optimized structure and electronic possessions**

The optimized structures of CuO clusters and (G– CuO models) are shown in Fig. 3. The adsorption of guanine phenomenon was understood from the following discussion. The calculated HOMO-LUMO energies of CuO and G-CuO clusters were shown in Table; 1. HOMO-LUMO energy gap values are decreasing with increasing size of the cluster. The electronic properties of CuO and G-CuO clusters are calculated from the highest occupied molecular orbital (HOMO) and lowest unoccupied molecular orbital (LUMO). Here HOMO acts as electron contributor and LUMO act as electron acceptors. Fig.5 shows the Electron distribution plots for HOMO of (a) G–$Cu_2O_2$, (b) G–Cu3O3,(c) G–$Cu_4O_4$ (R), (d) G–Cu4O4 (W) and LUMO of (e) G– $Cu_2O_2$, (f) G–$Cu_3O_3$, (g) G–$Cu_4O_4$ (R), (h) G–$Cu_4O_4$ (W). The red color shows positive nucleophilic and green color is revealed negative nucleophilic.

The electrons are spread over the copper oxide clusters except in G-$Cu_4O_4$ (W) in the HOMO energy level. But in the LUMO energy level, the electron distributions are uniformly spread over in the guanine. The HOMO-LUMO values of G-$Cu_2O_2$ cluster is **4.35**eV and hence this is the most favoring electronic structure**.** Further the first excited state of the LUMO is nearly uniformly spread thorough the CuO clusters except in G-$Cu_2O_2$. The large HOMO-LUMO gap implies that the structures are chemically inert because it is unfavorable to

  

electrons are added to higher LUMO level or to take away electrons from a lower HOMO level.[25]

**Fig: 2 Electronic Density of state plots (DOS) for CuO clusters (a) $Cu_2O_2$, (b) $Cu_3O_3$ (c) $Cu_4O_4$ (R) (d) $Cu_4O_4$**

The clusters like ((a) $Cu_2O_2$ (b) $Cu_3O_3$ (c) $Cu_4O_4$ (R) and (d) $Cu_4O_4$ (W)) are containing Cu and O atoms which are interact to five member guanine ring($N_1$) (Fig;3) like (a) G-$Cu_2O_2$, (b) G-$Cu_3O_3$ (c) G-$Cu_4O_4$ (R) and (d) G-$Cu_4O_4$ (W)) respectively . In which (G-N) is bond distance corresponding to **1.95(Å), 1.95(Å), 1.96 (Å) and 1.98(Å).**The bond distance is shorter for G-$Cu_2O_2$ (1.95$A^0$) when compared than G-CuO clusters. The energy gap values are slightly decreases as in G-$Cu_2O_2$ (**4.35eV**)> G-$Cu_4O_4$ (R) (**1.63eV**)> G-$Cu_4O_4$ (W)) (**1.36 eV**)> and G-$Cu_3O_3$(**0..27eV).**This is clearly shown in (Fig.2&4) DOS spectra of the Cuo and G-CuO clusters.

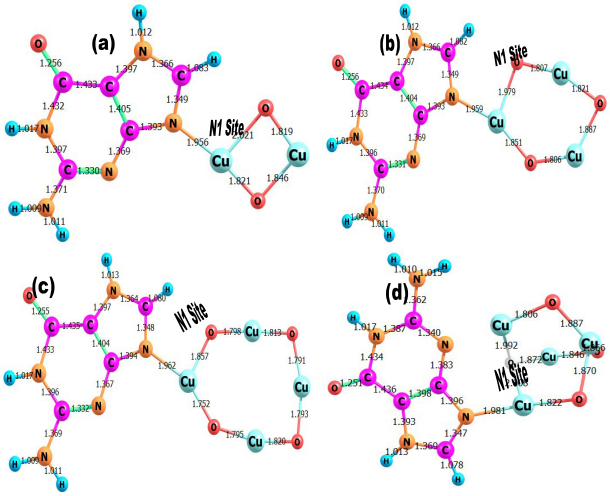


**Fig: 3 Models for four optimized structures of G–CuO clusters (a) G-$Cu_2O_2$, (b) G-$Cu_3O_3$ (c) G-$Cu_4O_4$ (R) and (d) G-$Cu_4O_4$(W)**

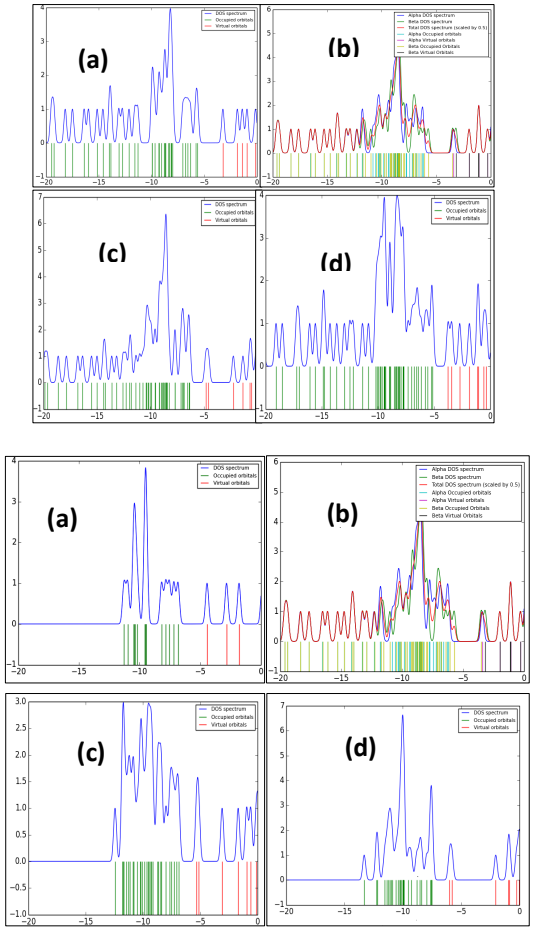


**Fig: 4 Electronic Density of state plots (DOS) for G-CuO clusters (a) G-$Cu_2O_2$, (b) G-$Cu_3O_3$ (c) G-$Cu_4O_4$ (R) (d) G-$Cu_4O_4$**

The binding energy value of G- CuO cluster are designed by the formula BE = $[[(n*E_{(Cu)}+ n*E_{(O)}+n*E_{(G]}- n*E_{(G-CuO)}]/n$ Where n is the number of atoms, $E_{(Cu)}$ is corresponding energy of Cu, $E_{(O)}$ is corresponding energy of O, $E_{(G)}$ is the energy of guanine and $E_{(G-CuO)}$ is the energy of guanine doped Copper oxide cluster.[26] The order of binding energy is slightly increases viz G-$Cu_2O_2$(1.90(eV) < G-$Cu_4O_4$ (R) (1.63(eV) < G-$Cu_3O_3$(2.12 (eV) <G-$Cu_4O_4$ (W)2.17(eV). (Table; 1) From the above values it is concluded that the most stable structure is G-$Cu_4O_4$ (W) among the

  

studied G-CuO clusters. In the CuO Clusters, oxygen atom bearing negative charge and in acting as donor and Cu atom bearing positive charge acting as an acceptor. Here the G-CuO clusters the atoms of N, O exhibit negative charge which are acting as donor atoms and the remaining H and Cu atoms have positive charge and it acting as acceptors as shown in Table: 3. Mulliken charges also used to clarify the stability of clusters. High value of Mulliken charges between $Cu_1$ (0.757) and $N_{15}$ (-0.648) exhibit is a weak bond interaction occurred between Cu-N in the G-$Cu_4O_4$ (W) cluster shown in (Table ; 3). It is confirmed that the electron population is rich in the above clusters. The Eg value of guanine (4.88eV) is marginally reduced, after the addition of the CuO clusters. The observed reduction is 10.8% [G–$Cu_2O_2$], 94.4% [G–$Cu_3O_3$], and 66.5% in the case of[G–$Cu_4O_4$(R)] and72.1% [G–$Cu_4O_4$ (W)].

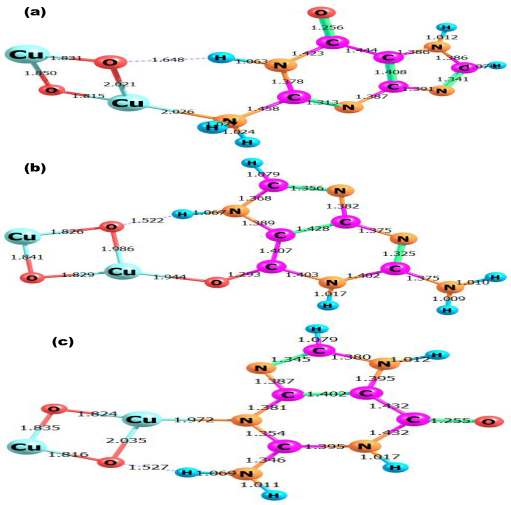

**Fig: 5 Models for optimized structures of G–CuO clusters at different site (a) $NH_2$, (b) C=O, (C)**

### 3) FT-IR Analysis

The representative FTIR spectra **(Figure. 6 a, b)** of the synthesized CuO and G-CuO nano material shows infrared peaks around 603 $Cm^{-1}$ which could be attributed to the monoclinic structure of CuO[27] The absorption bands observed at 604 and 512 $cm^{-1}$**(Fig.7b)** were assigned to the stretching of Cu-O nanoparticles.[28,]The vibration peaks 3420 $cm^{-1}$ indicates the presence of the hydroxide group in the sample.

This may be due to the water attached to the surface of the CuO nano particles, which is also one of the byproducts of the reaction and can be removed by further heating. The metal–oxygen bond is observed at 1380 $cm^{-1}$ (M-O rocking in plane) and at 2920 $cm^{-1}$ (M-O rocking out of plane) indicates the formation of CuO from copper Chloride. Generally absorption bands of metal oxide appears below 1000 $cm^{-1}$ that take place from inter atomic vibrations; the several peaks observed from 1120-1700 $cm^{-1}$ are due to C=O,C=N,C-C,C=C, stretching vibrations Fig (8b, c). The C=O peak observed at 1700 and 1670 $cm^{-1}$ as well as the broad absorption band observed at 3320, 3120, 2910 $cm^{-1}$ due to C-H,N-H,O-H stretching. The Cu–N band is formed at 480$cm^{-1}$.

**Fig.7** Shows the theoretical IR spectra of CuO and G-CuO clusters viz., The corresponding dominant peaks for IR shift in 600 $Cm^{-1}$($Cu_4O_4$(W)) while in $Cu_2O_2$ and $Cu_4O_4$ (R) shift appeared for 180$Cm^{-1}$ to 300$Cm^{-1}$ respectively. For G–CuO clusters the Cu–N

  

stretching vibration peaks are between 20–40 $cm^{-1}$ and 600–750 $cm^{-1}$.The absorption peaks of C=C, C–C, C=O and N–H are appeared at 1500–1800 $cm^{-1}$. From the computed values and comparison between the experimental IR values for CuO. It's concluded wurtzite structure of copper oxide is most favor cluster.

### 4) FT-RAMAN analysis

Investigation of FT-Raman spectra of CuO and G–CuO mixture are given in **Fig. 8.** CuO is monoclinic (space group $C_{2h}^6$ [$C_2/C$) on two molecules in the unit cell [29]. The CuO vibrational properties are calculated by group theory and by the following semi-empirical formula which indicates 12 phonon branches remaining to the f primitive cell in the four atoms. The zone center modes got out from group analysis

$\Gamma_{vibr}$ =Ag+2$B_g$+ 4Au+5Bu

**Fig. 8 (a)** shows are presence of 3 (Au + 2Bu) modes and 4Au + 5Bu + Ag + 2Bg symmetries with (9) zone-center optical phonon modes. Though, three Raman active

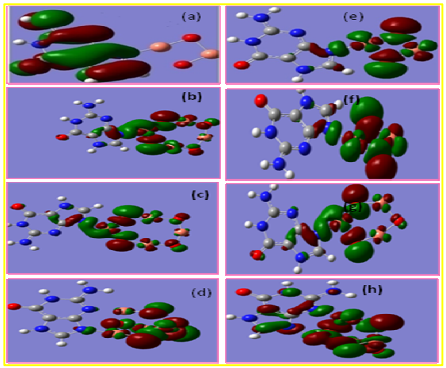


**Fig:6 Electron distribution plot for HOMO**

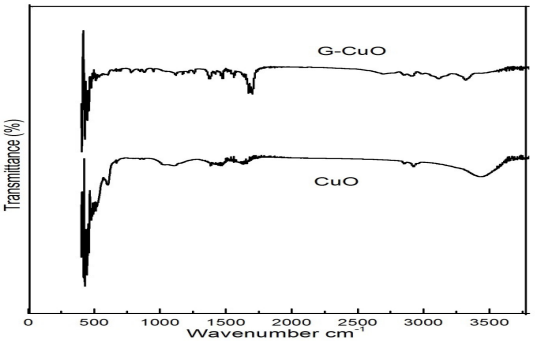


**Fig: 7** IR spectra for (a) CuO (b) G-CuO

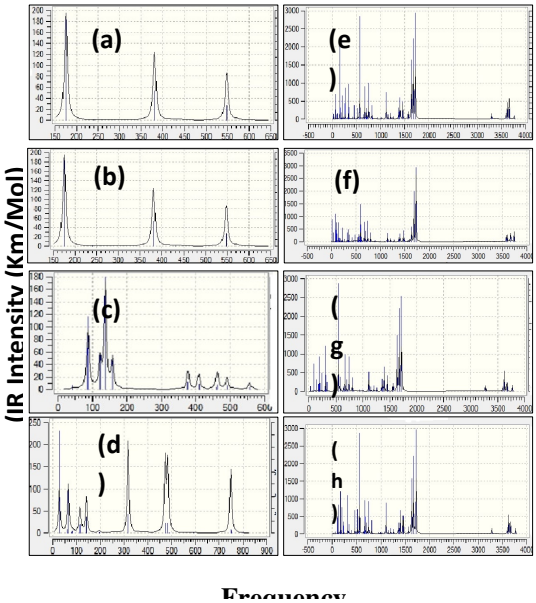


**Fig:8** Simulated IR spectra for CuO and G–CuO clusters (a) $Cu_2O_2$, (b) $Cu_3O_3$ (c) $Cu_4O_4$ (R) (d) $Cu_4O_4$ (e) G-$Cu_2O_2$, (f) G-$Cu_3O_3$ (g) G-$Cu_4O_4$ (h) (d) G-$Cu_4O_4$

symmetry modes Ag+2Bg are situated at peak positions of 293 (Ag), 347(2Bg) and 627 cm-1 (2Bg).[30] The IR active modes are continuing six (3Au + 3B u). Raman modes of Bg is revealed, atom of oxygen moved towards the b-direction for Ag and Bg modes upright towards the B-axis. The infrared active modes were demanding the

  

movement of Cu and O of both atoms. The induced dipole moments of Au modes are alongside the B-axis and Bu modes to vertical axis. The Raman peak observed at 293 $cm^{-1}$ is assigned for CuO non polar optical phonons of the Ag mode, which is one of the feature peaks of wurtzite CuO **(Fig. 9d).**

Raman spectra of G-CuO the line at 630 $cm^{-1}$ shown **Fig. (8 b)** in the RS, This line is indicate that the symmetric stretching vibration of the six- membered ring and agree with a line familiar to all purines close to 725 $cm^{-1}$. The very weak band appears at 824 $Cm^{-1}$ which represents, the formations of weak wander walls force between the Cu-N bond. The absorption band appeared over at 1000 $cm^{-1}$ comprise generally in plane modes, which confirms all are Raman active.The out-of- plane bending vibrations of C=H are powerfully coupled vibrations and band appeared in the range at 1000–750 $cm^{-1}$. A delicate band coincides along the stretching vibrations of carbonyl band appeared at 1680 $cm^{-1}$.

The simulated Raman spectrum shows in fig.10 CuO and G - CuO clusters, the most intense peak appearsat300 to 625 $Cm^{-1}$. Only three symmetry modes (Ag+2Bg) are Raman active located at peak positions of 293 (Ag), 347 (2Bg) and 627 cm-1. For G - CuO clusters the spectral region at 1000–1800 $cm^{-1}$ contains mostly in-plane modes, all are Raman active. The very weak band appears at 823 $Cm^{-1}$ in Cu4o4 (W) cluster. The FT-IR and FT-RAMAN spectrum of guanine is shown in **Fig. 8c** and **10c**. From above observational data, the FT-IR spectrum range occurs at (1600 to 512 $cm^{-1}$) in the G–CuO composite as equate with the guanine molecule. But slightly difference occurring in the FT-RAMAN spectra. Because observational information is interest to physisorption and which has been induce weak bond between guanine – CuO interactions. Finally DFT calculation results are preferential.

### 5) HR-SEM analysis and Elemental mapping

The SEM micrographs of the synthesized CuO and G-CuO are shown in the **Fig.10.** It seems that the particles were aggregated in CuO and form a cluster. The SEM micrographs of G-CuO (Fig: 10) shows as they are mainly agglomerated. Spherical shaped morphology is determined from the micrograph of (Fig.10) The average size of the copper oxide nano particle size is 25.2 nm. After adsorption to guanine in CuO, the nano particle size is increased. The G-CuO composite material size is 26.10 nm.The Dried powder of the sample

  

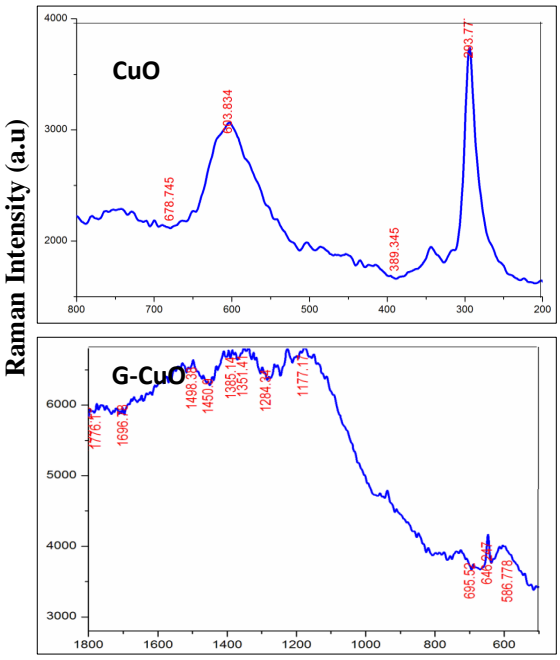


**Fig:9** Raman spectra for CuO

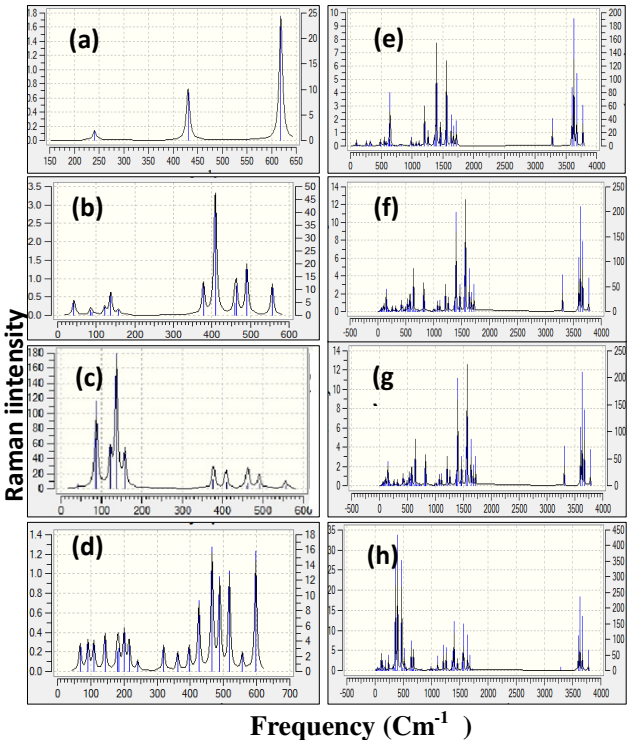


**Fig:10** Simulated Raman spectra for CuO and G–CuO clusters (a) $Cu_2O_2$,

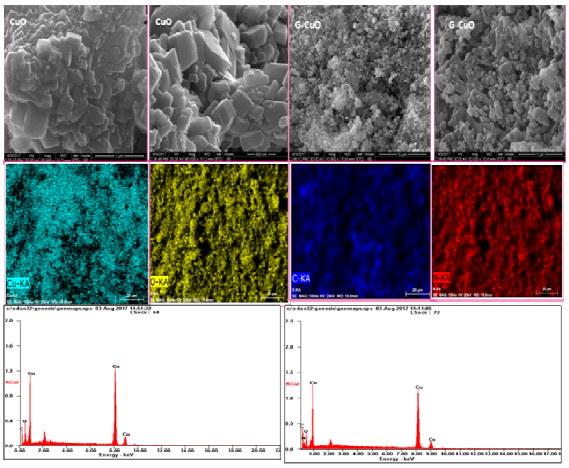


**Fig: 11 HR-SEM, EDAX and Elemental mapping images of (a)**

of CuO was analyzed by EDX. The peaks confirmed the presence of Cu and O atoms present in the CuO nano particles in **Fig .12(c, d).** The atoms of O, N and C are present in the G - CuO composite material. The high intense peak is appeared at 6 KeV. The demonstration of selected Cu,O,C and N elements were confirmed by EDAX and elemental mapping analysis.

### 6) UV-Vis absorption spectrum

UV-visible absorption spectrum of as synthesized CuO and G-CuO shows in **Fig.11.** The absorption peak of CuO appeared at 204,260 nm. Through, UV–Vis results, We have clarified the transfer in the band gap assign on the crystallinity of CuO, which shows a greater shift compared with that of the bulk (6.07,4.76eV) due to the size effect [31].On doping the band gap energy become reduced. The absorption spectra of guanine doped CuO

  

composite material show evidence of two complex band systems.

The band energy shows at 244nm and 274nm are depending with electronic transitions complex at 5.08eV and 4.52 eV. The absorption peak at 265 nm shows existence of CuO. A broad band at 314 nm (4.03eV) is attributed for guanine molecule Fig 11 (b, c). Furthermore the band gap energy of guanine is marginally decreased due to adsorption on CuO nano particles. Regarding theoretical verification of the guanine Eg values are become 51.7% [G–($Cu_4O_4$W) Further these nanoparticles can be used in semiconductor devices such as modulators, photo amplifiers for optical fiber communication system. For Copper and oxygen atom paramagnetic and ferromagnetic moments increases with decreasing size. The role of oxygen vacancies is corresponding to the generation of free carrier mediating ferromagnetism between copper spins.

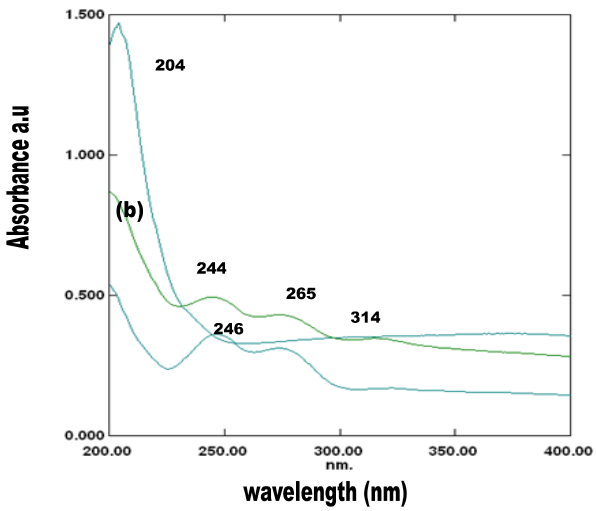


**Fig: 12 UV-visible spectra for (a) CuO , (b) G–CuO and (c) guanine**

## IV. CONCLUSIONS

Adsorption and physical interactions were carried out through experimental and DFT calculations. Guanine molecules are adsorbed on the surface of the copper oxide nanoparticle of size 26.10 nm. We have investigated electronic structure and stability of CuO and G-CuO clusters. We concluded that among the clusters, the favored stability and electronic structures are $Cu_4O_4$ (R), G-$Cu_4O_4$ (W) and Cu2O2, G-$Cu_2O_2$ respectively. Further our theoretical calculation shows the HOMO-LUMO energy gap values of G-$Cu_2O_2$ cluster is **4.35**eV and hence this is the most favored electronic structure**.** Electronic structure of guanine interacting with $Cu_2O_2$ cluster at different sites viz, $NH_2$, N, O site were studied and it is identified that N site of guanine is the most favored reactive site for the adsorption. The high value of Mulliken charges is supported physisorption is occurred within $Cu_1$ (**0.757)** and $N_{15}$ (-**0.648**) in the G-$Cu_4O_4$ (W) cluster. All interpretation prefer for the interaction of the G-$Cu_4O_4$ (W) nano particle surface. The experimental FT-IR and FT-Raman is in good agreement with DFT results. This study of bio - nano metal oxide interactions have numerous applications in industry.

## V. REFERENCE

**1.** M. J. G. Pacheo , J. E. Morales-Sanchz, J .Gernandez and F. Ruiz F., *Material Letters.* 64, 1361 **(2010).**

  

2. Y. X i, C.Hu, P.Gao, R .Yang, E.X, Wang and B .Wan, *Material Science and Engineering B.* 166, 113 **(2010)**.
3. Y,A.He . *Materical Research Bull* . 42, 190 **(2007)**.
4. M. Vaseem, A. Umar, Y. B. Hahn, D. H. Kim, K. S. Lee, J. S. Jang, and J. S. Lee, **.** *Bull. Mater.Sci*. 10, 11 **(2008)**.
5. A.Aslani, V.Oroojpour ,*Physica B: Condensed Matter.* 406, 144 **(2011)**.
6. C.Wang, W. Zeng, Zhang, H. *J Mater Sci: Mater Electron.* 25, 2041 **(2014**).
7. R. Srivastava, M. U. AnuPrathap, and A. R. Kore, *Physicochem. Eng. Aspects*. 392, 271 **(2011)**.
8. Y. Hong-Ying, X. Miao-Qing, S. H. Yu, and G. C. Zhao, *Int. J. Electrochem. Sci.* 8, 8050 **(2013)**.
9. J. Y. Xiang, J. P. Tu, L. Zhang, Y. Zhou, X. L. Wang, and S. J. Shi, *J. Power Sources.*195, 313 **(2010)**.
10. J. Hong, J. Li, and Y. Ni , *J. Alloys Compd.* 481, 610 **(2009)**.
11. Y. K. Kim, D. H. Riu, S. R. Kim, and B. I. Kim, *Mater. Lett*. 54, 229 **(2002)**.
12. Z. Yang, J. Xu, W. Zhang, A. Liu, and S. Tang, *J. Solid State Chem.* 180, 1390 **(2007)**.
13. M. M. Feeney, J. M. Kelly, A.B Tossi, A.K. Mesmaeker, J.P. Lecomte, *J. Photochem. Photo biol. B.* 23, 69 **(1994).**
14. Jean Cadet, J. Richard Wagner, Vladimir Shafirovich, and E. Nicholas , *Int J Radiat Biol.* 90(6): 423 **(2014).**
15. S.Nations, M.Long, M.Wages, J.D.Maul, C.W.Theodorakis, G.P.Cobb, *Chemosphere.* 135, 166 **(2015).**
16. F.Perreault, S.PMelegari,.; C.H.; Da Costa, A.L.d.O.F.Rossetto, R.Popovic, W.G Matias,. Genotoxic effectsof copper oxide nano parnanoparticles in Neuro 2A cell cultures. *Sci. Total Environ,* 441, 117 **(2012).**
17. KM. Reddy, K. Feris, J.Bell, DG .Wingett, C Hanley, A Punnoose. *Appl Phys Lett.* 90:2139021-3 **(2007).**
18. AJ. Huh, YJ. Kwon , *J Controll Release.* 156, 128 **(2011).**
19. R Dastjerdi, M. Montazer, *Colloids Surf B Bio interfaces.* 79, 5 **(2010).**
20. K.Blecher, A.Nasir, A.Friedman, *Virulence.* 2, 395 **(2011).**
21. PK.Stoimenov, V.Zaikovski, KJ. Klabunde , *J Am Chem Soc.* 125, 12907 **(2003)**.
22. V. L. Chandraboss , B. Karthikeyan and S. Senthilvelan, *phys,chem..chem.phys.* 16, 23461 **(2014).**
23. G.L.Wang, J.C.Huang, S. L Chen, Y. Y Gao, D. X Cao, *J. Power Sources.* 196, 5756 **(2011)**.
24. H. X Zhang, M. L.Zhang, *Mater. Chem. Phys.* 108, 184 **(2008)**.
25. R. N. Nickolov, B. V.Donkova, K. I.Milenova, D. R. Mehandjiev, *Adsorpt. Sci. Technol.* 24, 497 **(2006).**
26. V.Saravanakannan, T.Radhakrishnan, *Research Journal of Pharmaceutical,*


  

*Biological and Chemical Sciences,* 4(4), 589 **(2013)**.

**27.** V.Nagarajan; R.Chandiramouli, *Int.J. ChemTech Res.,* 6(1), 21 **(2014)**.

**28.** V.Saravanakannan, T.Radhakrishnan, *Int. J. ChemTech Research*. 6, 3611 **(2014).**

**29.** G.Igel, U.Wedig. M.Dolg, P.Fuentealba, H.Preuss H.Stoll, R.Frey, *Journal of Chemical Physics.* 81, 2737 **(1984)**.

**30.** C. W.; Claudia, J. B.Enrique, *Acta farmaceutica bonaerense*, *Argentina.* 23, 339 **(2004).**

**31.** H.Goldstein , D Kim, P.Yu,. *Phys Rev B.* 41, 192 **(1990)**.

Table:1 Calculated HOMO Energies ($E_{HOMO}$), LUMO energies ($E_{LUMO}$), HOMO-LUMO energy gap (Eg), distance of Cu-N ($A^0$), scaled energies ($E_s$) and binding energies ($E_b$) using b3lyp/lanl2dz method

| S.No | Structure | $E_{HOMO}$( eV) | $E_{LUMO}$( eV) | (Eg) eV, | Distance of Cu–N (A) | $E_g$( eV) | $E_b$ (eV) |
|---|---|---|---|---|---|---|---|
| 1 | $Cu_2O_2$ | -4.35 | -6.80 | 2.45 | - | 13.78 | -3,691.15 |
| 2 | $Cu_3O_3$ | -9.80 | -9.77 | 0.03 | - | 22.5 | -3,691.85 |
| 3 | $Cu_4O_4$ (R) | -7.34 | -5.98 | 1.36 | - | 31.02 | -3,692.12 |
| 4 | $Cu_4O_{4(W)}$ | -6.80 | -5.17 | 1.63 | - | 29.66 | -3,691.85 |
| 5 | G - $Cu_2O_2$ | -7.34 | -2.99 | 4.35 | 1.95 | 1.90 | |
| 6 | G- $Cu_3O_3$ | -9.52 | -9.25 | 0..27 | 1.95 | 2.12 | |
| 7 | G- $Cu_4O_4$ (R) | -6.29 | -4.62 | 1.63 | 1.96 | 1.63 | |
| 8 | G- $Cu_4O_{4(W)}$ | -4.89 | -3.53 | 1.36 | 1.98 | 2.17 | |
| 9 | Guanine | -6.09 | -1.23 | 4.88 | | | |

Table: 2 Mulliken atomic charges of CuO clusters at the b3lyp/lanl2dz basis set

| Atoms ($Cu_2O_2$) | Atomic charges | Atoms ($Cu_3O_3$) | Atomic charges | Atoms ($Cu_4O_4$ (R) | Atomic charges | Atoms ($Cu_4O_4$ (W) | Atomic charges |
|---|---|---|---|---|---|---|---|
| $Cu_1$ | 0.574 | $Cu_1$ | 0.663 | $Cu_1$ | 0.620 | $Cu_1$ | 0.653 |
| $O_2$ | -0.574 | $O_2$ | -0.654 | $O_2$ | -0.622 | $O_2$ | -0.510 |
| $Cu_3$ | 0.574 | $Cu_3$ | 0.644 | Cu3 | 0.615 | $Cu_3$ | 0.590 |
| $O_4$ | -0.574 | $O_4$ | -0.645 | $Cu_4$ | 0.620 | $O_4$ | -0.658 |
| | | $O_5$ | -0.654 | $O_5$ | -0.638 | $O_5$ | -0.591 |
| | | $Cu_6$ | 0.646 | $Cu_6$ | 0.664 | $Cu_6$ | 0.512 |
| | | | | $O_7$ | -0.638 | $O_7$ | -0.548 |
| | | | | $O_8$ | -0.621 | $Cu_8$ | 0.553 |

\

  

Table:3 mulliken atomic charges of G-CuO clusters at the b3lyp/lanl2dz basis set

| Atoms ($G\text{-}Cu_2O_2$) | Atomic charges | Atoms ($G\text{-}Cu_3O_3$) | Atomic charges | Atoms ($G\text{-}Cu_4O_4$ (W) | Atomic charges | Atoms ($GCu_4O_4$(R) | Atomic charges |
|---|---|---|---|---|---|---|---|
| $N_1$ | -0.363 | $O_1$ | -0.587 | $N_1$ | -0.356 | $Cu_1$ | 0.620 |
| $C_2$ | -0.031 | $Cu_2$ | 0.540 | $C_2$ | -0.035 | $O_2$ | -0.574 |
| $N_3$ | -0.321 | $O_3$ | -0.660 | $N_3$ | -0.336 | $O_3$ | -0.562 |
| $C_4$ | 0.112 | $Cu_4$ | 0.666 | $C_4$ | 0.147 | $O_4$ | -0.644 |
| $N_5$ | -0.050 | $Cu_5$ | 0.465 | $N_5$ | -0.060 | $Cu_5$ | 0.473 |
| $C_6$ | 0.200 | $O_6$ | -0.657 | $C_6$ | 0.207 | $O_6$ | -0.682 |
| $N_7$ | -0.623 | $N_7$ | -0.359 | $N_7$ | -0.622 | $Cu_7$ | 0.459 |
| $N_8$ | -0.409 | $C_8$ | -0.042 | $N_8$ | -0.409 | $Cu_8$ | 0.522 |
| $C_9$ | 0.153 | $N_9$ | -0.330 | $C_9$ | 0155 | $N_9$ | -0.357 |
| $O_{10}$ | -0.285 | $C_{10}$ | 0.136 | $O_{10}$ | 0.277 | $C_{10}$ | -0.090 |
| $C_{11}$ | 0.122 | $N_{11}$ | -0.057 | $C_{11}$ | 0.123 | $N_{11}$ | -0.285 |
| $Cu_{12}$ | 0.575 | $C_{12}$ | 0.202 | $Cu_{12}$ | 0.757 | $C_{12}$ | 0.351 |
| $O_{13}$ | -0.520 | $N_{13}$ | -0.623 | $O_{13}$ | -0.667 | $N_{13}$ | -0.295 |
| $Cu_{14}$ | 0.466 | $N_{14}$ | -0.409 | $Cu_{14}$ | 0.497 | $C_{14}$ | 0.377 |
| $O_{15}$ | -0.543 | $C_{15}$ | 0.153 | $O_{15}$ | -0.662 | $N_{15}$ | -0.648 |
| $H_{16}$ | 0.354 | $O_{16}$ | -0.281 | $Cu_{16}$ | 0.517 | $N_{16}$ | -0.414 |
| $H_{17}$ | 0.333 | $C_{17}$ | 0.121 | $O_{17}$ | -0.609 | $C_{17}$ | 0.158 |
| $H_{18}$ | 0.365 | $H_{18}$ | 0.356 | $Cu_{18}$ | 0.512 | $O_{18}$ | -0.261 |
| $H_{19}$ | 0.324 | $H_{19}$ | 0.338 | $O_{19}$ | -0.605 | $C_{19}$ | 0.124 |
| $H_{20}$ | 0.340 | $H_{20}$ | 0.366 | $H_{20}$ | 0.359 | $H_{20}$ | 0.363 |
| | | $H_{21}$ | 0.325 | $H_{21}$ | 0.324 | $H_{21}$ | 0.282 |
| | | $H_{22}$ | 0.342 | $H_{22}$ | 0.369 | $H_{22}$ | 0.395 |
| | | | | $H_{23}$ | 0.327 | $H_{23}$ | 0.331 |
| | | | | $H_{24}$ | 0.344 | $H_{24}$ | 0.353 |

  

  

  